Modern Research in Catalysis, 2015, 4, 68-77
Published Online July 2015 in SciRes. http://www.scirp.org/journal/mrc
http://dx.doi.org/10.4236/mrc.2015.43009

Effect of Potassium on Sol-Gel Cerium and Lanthanum Oxide Catalysis for Soot Combustion

Daniela Salinas[1*], Gina Pecchi[1], Vicente Rodríguez[1], José Luis García Fierro[2]

[1]Department of Physical Chemistry, Faculty of Sciences, University of Concepcion, Concepcion, Chile
[2]Institute of Catalysis and Petrochemistry, ICP-CSIC, Cantoblanco, Madrid, Spain
Email: [*]dasalinas@udec.cl

Received 4 June 2015; accepted 13 July 2015; published 17 July 2015

Abstract

The catalytic activity in the soot combustion is reported for a series of potassium-promoter alumina supported catalysts prepared by the sol-gel method to be used in the catalytic combustion of soot. The studied systems correspond to CeO_2-Al_2O_3 and La_2O_3-Al_2O_3 with charges of 3 and 5 wt% of CeO_2 and La_2O_3. Potassium impregnation is performed to reach 3 atoms of K per nm^2 of the mixed oxide. The effect of the potassium incorporation increases its reducibility, decreases the surface area and forms a new type of oxygen that is stronger than the oxygen in mixed oxides with similar chemical nature. The existence of potassium oxides, K_2O and oxygen responsible for the vacancies and/or lattice defects (O^{2-}) are related to good catalytic activity. Additionally, the presence of alkali affects the structural and textural characteristics of the catalyst, promoting the catalytic activity in soot combustion.

Keywords

Sol-Gel, Potassium, Cerium, Lanthanum, Soot Combustion

1. Introduction

It is generally known that in the oxidation of hydrocarbons, the volatile organic compounds (VOCs), the particulate matter such as soot, and the emission of NO_x species into the atmosphere are harmful to people and environment [1]. An alternative for the control of these species is catalytic combustion [2]-[8]. The stabilization of the emission levels of these materials is increasingly strict, and new catalysts have been developed to meet the requirements of these new technologies. Soot is a particulate material resulting from the incomplete combustion

[*]Corresponding author.

How to cite this paper: Salinas, D., Pecchi, G., Rodríguez, V. and Fierro, J.L.G. (2015) Effect of Potassium on Sol-Gel Cerium and Lanthanum Oxide Catalysis for Soot Combustion. *Modern Research in Catalysis*, **4**, 68-77.
http://dx.doi.org/10.4236/mrc.2015.43009

of diesel fuel that remains in the filters of vehicle engines, causing serious health problems [9]. An alternative is to burn this particulate material [7] [9]. The catalyst deposited in the ceramic filters could oxidize the soot, reducing its emission into the atmosphere. However, the temperatures at which the gases emitted into the atmosphere are cooled between 300˚C and 400˚C, coal is burned at temperatures that range between 500˚C and 600˚C. Therefore, the catalysts used in the catalytic combustion of soot must be capable of presenting catalyst activity at low temperatures [10].

An important number of catalytic formulations have been developed in this field, including oxides [11]-[14], perovskites [9] [15]-[17], spinels [18] and metals [19]. The range of metals refers to the use of noble metals [20] which are not favorable for commercial use due to their high cost. However, metallic oxides [21]-[23] used as catalysts are more favorable as the atomic number of the metal increases because of the promotion effect with alkali materials [24]. Additionally, K^+ could lower the unsaturation of oxide anion coordination and the mobility of atoms. It is well known that the catalytic combustion of soot is favored by basic catalysts [24]; thus, to enhance the catalytic properties of K-supported catalysts, the addition of CeO_2 and La_2O_3 is proposed to improve and enhance the catalytic activity of the support metal oxides.

The catalysts in this study have been impregnated with potassium. Additionally, the thermal stability, redox properties and wide application of metallic oxides are widely recognized. The incorporation of two metals into the oxide allows materials to be generated with different structural and electronic properties [25]. Within these properties, the morphological and valence changes are highlighted, as well as possible vacancies that originate in the material or the change in the chemical nature of the elements. CeO_2 has been considered because of its redox properties and its great affinity for the adsorption of oxygen [26]-[28], which could favor the basic characteristics of the catalyst. Furthermore, the great capacity of the cerium to admit modifications in both the surface and in the bulk of the material is also highlighted. La_2O_3 has been chosen because of its recognized thermal stability, and the presence of La^{3+} confers a basic character to the catalyst. The aim of this work is to study the different effects produced when K is supported on two different mixed oxides: CeO_2/Al_2O_3 and La_2O_3/Al_2O_3. The samples are prepared by the co-gelation of the catalyst precursors to avoid sintering and the induction of a stronger interaction between the oxides.

2. Experimental Analysis

2.1. Preparation

The sol-gel La_2O_3-Al_2O_3 and CeO_2-Al_2O_3mixed oxides were prepared using tri-sec-aluminum butoxide and the corresponding acetylacetonates of cerium and lanthanum to achieve 3 and 5 wt% of CeO_2 and La_2O_3. The gelling reaction was accomplished in 1 h under reflux at 70˚C and in presence of distilled water and 2-buthanol, maintaining water to 2-buthanol molar ratio of 1:4. The obtained gels were dried in air at 110˚C and calcined at 600˚C for 6 h. The potassium was impregnated with an aqueous KNO_3 and dissolution dried at 100˚C; it was again calcined at 600˚C for 4 h. The potassium content was fixed in three K atoms per nm^2 of support. Considering the similar specific area values of the mixed oxides, the K content was around to 9 wt% in the prepared catalysts.

2.2. Characterization

The calcined sol-gel mixed oxides and K-supported catalysts were characterized by means of AAS in a Perkin Elmer 3100 absorption spectrometer and N_2 adsorption isotherms at 77 K using Micromeritics ASAP 2010 equipment. XRD was performed in a Rigaku diffractometer, using CuK_α (λ = 0.15406 nm) as a radiation source and an Ni filter. For the TPR experiments, 0.500 g of the sample was reduced under an H_2flow up to 700˚C in a Micromeritics TPR/TPD 2900 system equipped with a thermal-conductivity detector. Programmed thermal desorption profiles of O_2 and NH_3 were performed prior to cleaning the samples in He to a flow of O_2 for 1 h at 700˚C and then cooled at room temperature. After reaching room temperature, the desorption profile was detected at a heating rate of $10^{\circ}C \cdot min^{-1}$. The XPS measurements were performed in a VG Thermo Escalab 200R spectrometer equipped with an MgK_α radiation source. Prior to the analysis, the samples were degasified at 300˚C for 1 h in the spectrometer chamber. As reference, the peak of C1s occurred at 284.8 eV.

2.3. Catalytic Activity

The evaluation of the catalytic activity for soot combustion was studied using carbon black (CB) as the soot

model. The catalyst and CB mixture for the assessment of the catalytic activity was prepared by mixing 4 mg of CB and 16 mg of catalyst in tight contact. The catalytic oxidation of the soot was conducted in a thermogravimetric apparatus (Netzch 409 PC) with 7.5 mg of the mixture heated in a 180 mL·min^{-1} flow of 12%O_2/He at 10˚C·min^{-1} up to 800˚C. The temperature at which combustion occurs at the maximum rate, denoted as T_m, was used as the measure of the catalytic activity. The stationary point method was used to calculate the apparent activation energy. Typically, samples of the catalysts and CB mixtures in tight contact were heated at four different heating rates in 180 mL·min^{-1} of 12%O_2/He in a thermogravimetric equipment.

3. Results and Discussion

3.1. Specific Area

The specific BET areas are summarized in **Table 1**. As expected, the sol-gel method generated materials with high surface area, which decreased when the alkali metal was added [24] [29]. Although the impregnation of 10 wt% of a metal could decrease the surface area of the support, the larger decreases illustrated in **Table 1** were a consequence of the chemical behavior of potassium. Previous studies of this behavior indicate that, independent of the nature of support, the impregnation of potassium decreases the surface area over 50% of its total extent [24] [30]. The results of **Table 1**, corresponding to the reported effect, greatly decrease the S_{BET} values for the K5%La_2O_3-Al_2O_3 catalyst, in which the area decreases to a value as low as 35 $m^2 \cdot g^{-1}$, corresponding to 90% of the mixed oxide. In the other catalysts the decreases were approximately 85%.

3.2. XRD Diffraction

The diffraction profiles of the mixed oxides and the K-supported catalysts are shown in **Figure 1**. At the top of **Figure 1**, the diffractograms correspond to the K-supported catalysts, and the bottom diffractograms correspond to the mixed oxides. It is seen that the addition of cerium or lanthanum precursor to the aluminum alkoxide during the gelation step leads to rather amorphous solids. Regarding to the CeO_2-Al_2O_3 mixed oxides, the CeO_2 (JPDF: 43-1002) phase is clearly identified, increasing with CeO_2 loading. A different behavior is observed in the La_2O_3-Al_2O_3 counterparts, in which no diffraction peaks attributed to La_2O_3 (JPDF: 22-0369) are detected. The explanation relates to the previous reports where lanthanum species are inserted into the pore alumina or no diffraction is detected because the lanthanum species are highly dispersed in the amorphous phases [2]. Thus, the observed trend indicates that the lanthanum species inserted into the alumina lattice and the cerium is deposited as surface patches on the alumina. However, only for the 5 wt% La_2O_3-Al_2O_3 is it possible to detect a diffraction line of La_2O_3, indicative that for 5 wt% of La_2O_3, the lanthanum species are well-dispersed and could form agglomerates. **Table 1** displays the detected phases for the mixed oxides and the K-supported catalysts. Moreover, the similar diffractograms of the mixed oxides and the K-supported catalysts indicate a high thermal stability of the sol-gel mixed oxides. With regard to the K-supported catalysts, the K content of ~9 wt% allows crystalline K species to be detected if they are in a low dispersion degree. No diffraction lines attributed to the K

Table 1. Surface area, pore volume, AAS K wt% and detected XRD phases of the support and K-supported catalysts.

Catalyst	S_{BET}, $m^2 \cdot g^{-1}$	V_{pore}, $cm^3 \cdot g^{-1}$	*K*, wt%	Detected XRD phases			
3%CeO_2-Al_2O_3	502	0.26	-	CeO_2	Al_2O_3	-	-
5%CeO_2-Al_2O_3	475	0.40	-	CeO_2	Al_2O_3	-	-
3%La_2O_3-Al_2O_3	486	0.53	-	-	Al_2O_3	-	-
5%La_2O_3-Al_2O_3	490	0.06	-	-	Al_2O_3	-	-
K/3%CeO_2-Al_2O_3	69	0.17	9.2	CeO_2	Al_2O_3	-	-
K/5%CeO_2-Al_2O_3	156	0.26	9.1	CeO_2	Al_2O_3	-	-
K/3%La_2O_3-Al_2O_3	116	0.35	9.2	-	Al_2O_3	-	-
K/5%La_2O_3-Al_2O_3	35	0.04	9.0	-	Al_2O_3	La_2O_3	K_2O

(–) indicates nothing was detected.

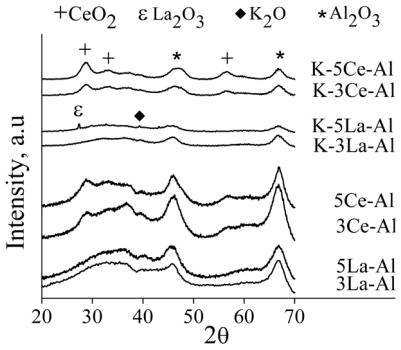

Figure 1. XRD spectra of the mixed oxides and K-supported catalysts.

species are detected, except for the larger La_2O_3 content in which only one diffraction line for a potassium species of K_2O (JPDF:77-2151) is detected. This diffraction peak of K_2O indicates lower potassium dispersion in this K/5% La_2O_3-Al_2O_3 catalyst.

3.3. Temperature Programmed Reduction (TPR)

Temperature-programmed reduction (TPR) profiles up to 700˚C are shown in **Figure 2**. The similarity of the reduction profiles of each series is noticeable. The absence of the well-defined reduction peak of the mixed oxides indicates practically irreducible solids.

The non-reducible behavior of the mixed oxides used as support, attributable to the reduction peak at ~500˚C, appear for the K-supported catalysts to the potassium species. Moreover, the large reduction peak of the K-supported catalysts confirms the presence of potassium; although its presence was not detected by XRD because of its high dispersion degree. For better insight into the reduction behavior, the total H consumption in the TPR profiles between 400˚C and 500˚C, which is a measure of the amount of K^+ species, is evaluated by deconvolution of the area under the curve using a Lorentzian peak, as shown in **Table 2**. The similar H consumption that corresponds to a ~25% reduction indicates a similar amount of reduced potassium. It is proposed that the lower the reduction temperature, the lowest the K-mixed oxide interaction. Thus, for the CeO_2-Al_2O_3 mixed oxides, the larger extent of cerium oxide as patches in 5%CeO_2-Al_2O_3 facilitate the alkali reduction at lower temperatures. The opposite effect is observed for the catalysts with lanthanum oxide, in which the reduction profiles indicate a reduction of the alkaline metal of the catalyst K/3%La_2O_3-Al_2O_3 at 511˚C, shifted towards higher temperatures; for K/5%La_2O_3-Al_2O_3, the catalyst presents the highest temperature of reduction.

3.4. O_2-Desorption Profile (O_2-DTP)

Figure 3 displays the evolution of oxygen during the temperature-programmed desorption (O_2-TPD) experiments, which is also closely related to the redox properties of the catalysts. The O_2-TPD profiles of the mixed oxides are similar, indicating the large extent of desorbed oxygen, as expected because of their large number of hydroxyl groups. With regard to the K-supported catalysts, both series display similar desorption profiles, attributed to the alkali presence, and confirm the presence of highly dispersed K species. The TPD-MS experiments confirm that the evolved gas and the He flow only contain oxygen; therefore, the deconvolution of the oxygen desorption curves using the Lorentzian peak shapes allow the amount of the different desorbed oxygen species to be calculated. In **Table 2**, the amount of desorbed oxygen for the desorbed temperature is displayed. For the La_2O_3-Al_2O_3 series, there are clear larger increases of desorbed oxygen in the K-supported catalysts compared to the mixed oxides. This behavior indicates that potassium allows oxygen to be withheld and contributes to the formation of surface oxygen with deeper interactions with K. For lower contents of La_2O_3, the oxygen is desorbed over 250˚C; however, for higher La_2O_3 content, the desorption temperature is displaced over 350˚C. This is in agreement with the results of TPR because at lower contents of La_2O_3, the potassium interacts with the support that allows for more oxygen desorption when compared to cerium catalysts. This corroborates the ease of CeO_2 to retain oxygen. Previous works have established that the desorption peak lower 400˚C are associated oxygen that is weakly bonded to the solid network [31]. Likewise, desorption at temperatures close to 500˚C is

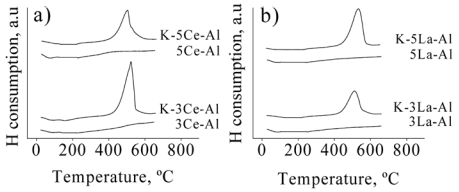

Figure 2. TPR profiles of the mixed oxides and K-supported catalysts.

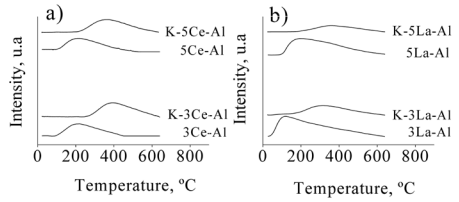

Figure 3. TPD-O_2 profiles of the mixed oxides and K-supported catalysts.

Table 2. TPR and O_2-DTP results for the support and K-supported catalysts.

Catalyst	T red, ˚C	H consumption µmol·g^{-1}	T desorption, ˚C	O desorbed µmol·g^{-1}
3%CeO_2-Al_2O_3	>600	0	400	350
5%CeO_2-Al_2O_3	>600	0	150	510
3%La_2O_3-Al_2O_3	>600	0	105	230
5%La_2O_3-Al_2O_3	>600	0	180	170
K/3%CeO_2-Al_2O_3	522	530	385	510
K/5%CeO_2-Al_2O_3	504	420	352	520
K/3%La_2O_3-Al_2O_3	511	450	320	870
K/5%La_2O_3-Al_2O_3	531	620	361	690

attributed to the strong oxygen bonds to the network [32]-[35]. Clearly, the incorporation of potassium allows oxygen to have more force than in solids without alkali. According to **Table 2**, the amount of desorbed oxygen is lower for the K-cerium catalysts.

3.5. XPS analysis

Table 3 compiles the respective binding energies (BE) of the core electrons of the elements. The C1s, O1s, Ce3$d_{5/2}$, La3$d_{5/2}$ and K 2$p_{3/2}$ core-level spectra were recorded for the K-supported catalysts. The C1s, O1s, Ce3$d_{5/2}$, La3$d_{5/2}$ and K 2$p_{3/2}$ core-level spectra were recorded for the K-supported catalysts. **Figure 4** shows the spectra for one representative catalyst, the K/5%La_2O_3-Al_2O_3. The C1s emission was used as reference. According to Praveen *et al.* [36] and Fleming *et al.* [37], the BE range of Ce between 875eV and 925 eV indicates a mixture of surface Ce^{3+} and Ce^{4+}. The obtained BE values of **Table 3** of Ce 3$d_{5/2}$ at 883.0 eV and Ce 3$d_{3/2}$ at 900 eV have a relationship with 13% and 12% of Ce^{3+} for the K/3%CeO_2-Al_2O_3 and K/5%CeO_2-Al_2O_3 catalysts, respectively. The presence of Ce^{3+}, poorly appreciated, associated with the surface anion vacancies could be a consequence of the removal of oxygen during the sample pretreatment.

The reported BE of La 3d between 830 eV and 870 eV [36] and La 3$d_{5/2}$ at 834.9 eV for surface La^{3+} indicates that the obtained values of 835.1 and 835.4 eV shifted towards higher BE, indicating the presence of only La^{3+}

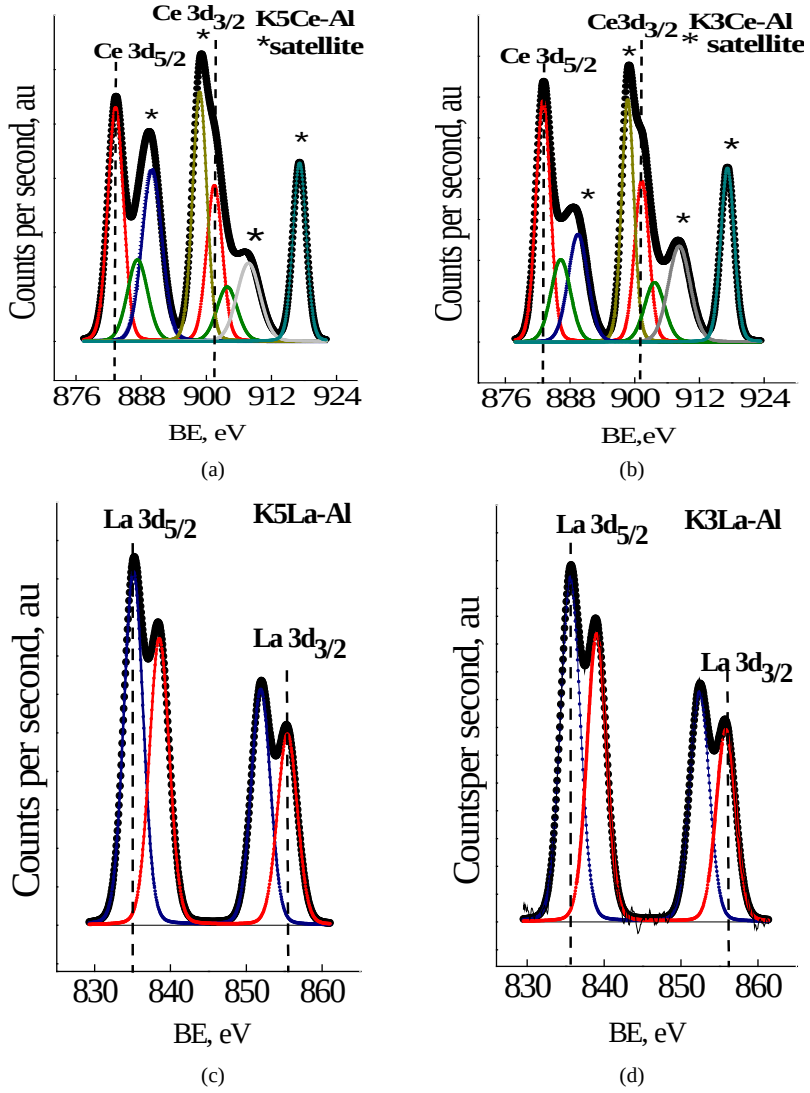

Figure 4. XPS data of the K-supported catalyst.

Table 3. Binding energies (eV) of the core levels for the K-supported catalysts.

Catalyst	Ce $3d_{5/2}$	La $3d_{5/2}$	O 1s	K $2p_{3/2}$
K/3%CeO_2-Al_2O_3	883.0 (13)	------	531.6	293.6
K/5%CeO_2-Al_2O_3	883.1(12)	------	531.7	293.8
K/3%La_2O_3-Al_2O_3	------	835.4	531.6	293.4
K/5%La_2O_3-Al_2O_3	------	835.1	531.5	292.8

( ) mean percentage of Ce^{3+} over the surface catalyst

[38]. This is the expected result considering no other stable oxidation state of lanthanum occurs when combined with oxygen. Thus, the corresponding BE of lanthanum in the La_2O_3-Al_2O_3 mixed oxides indicates a La^{3+}cation is partially inserted into the alumina lattice leading to a strong La-O interaction [39]. The O1s BE at 531.5 to 531.7 eV is associated with the weakly bonded surface species [32]. With regard to the surface K species, the BE at 293.4 to 293.8 eV is indicative of potassium in a cationic chemical environment (K δ^+) [30], present in 3 wt% La_2O_3, 3 wt% CeO_2 and 5 wt% CeO_2 content of the K catalysts. A different behavior is detected for the

K/5%La_2O_3-Al_2O_3, in which the BE decreases to 292.8 eV. This shift towards higher BE indicates more oxidized species, whereas the shifts towards lower BE are related with the surface deficit electronic density potassium species. According to the XRD spectra, the K_2O detected appears as a cationic chemical environment (K δ^+) when the potassium is similar to the K_2O species [28].

Figure 5 and **Figure 6** show the bulk and surface Ce/Al, La/Al and K/Al atomic ratios. It can be seen for both of the studied series that the higher surface values are indicative of the surface enrichment of Ce and La. Although, in the K-supported on the CeO_2-Al_2O_3 catalysts, the lower difference between the surface and bulk Ce/Al indicates a lower dispersion of CeO_2 on the Al_2O_3, easily detected by XRD. With regard to the La/Al, the larger differences between the surface and bulk values as well as the shifted of surface La^{3+} species support the hypothesis that surface K/5%La_2O_3-Al_2O_3 catalysts becomes La-enriched. Surface K/Al ratios are lower than the bulk ratios for both series with similar values for each series. The higher surface K/Al ratios for the K/CeO_2-Al_2O_3 catalysts indicate highly dispersed K species, in agreement with XRD. With regard to the La_2O_3-Al_2O_3 catalysts, the surface La-enrichment in the K/5% La_2O_3-Al_2O_3 catalyst by the larger inclusion of La^{3+} in the Al_2O_3 lattice may be the responsible for the presence of the K_2O phase, detected by XRD, and the large K dispersion compared to the K/3%La_2O_3-Al_2O_3.

3.6. Catalytic Activity

Figure 7 shows the DTG curves for the CB combustion of the K-supported catalysts. The catalytic activity is related to the temperature corresponding to the maximum of the DTG curve (T_m). Higher values of T_m indicate lower catalytic activity. The T_m values and the apparent activation energy (E_{act}) of the mixed oxides and the K-supported catalysts are summarized in **Table 4**. The T_m value for the uncatalyzed CB combustion was found to be 650˚C (not shown), relatively the same value as the corresponding mixed oxides without the alkali active phase (not shown). Thus, the decreases at approximately 200˚C in the T_m values for the K-supported catalysts indicate the catalytic effect of the alkali. Although **Figure 7** shows that there are no large differences in the K-supported catalysts, the 10˚C temperature decreases of the maximum reaction rate for the K/5%La_2O_3-Al_2O_3 catalysts can be explained considering the characterization results. Moreover, the apparent activation energy supports this feature. The apparent activation energies of the uncatalyzed reaction is 170 kJ·mol^{-1}, and E_{act} values from 108 to 81 kJ·mol^{-1} have been reported for soot combustion with potassium-lanthanum cobaltite catalysts [40]. The E_{act} of the mixed oxides is on the order of 137 to 145 kJ·mol^{-1}, so it decreases to 92 and 81 kJ·mol^{-1}

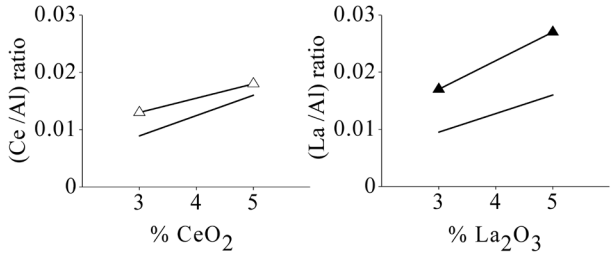

Figure 5. Atomic Ce/Al and La/Al ratios: (-) bulk; (Δ) cerium surface; (▲) lanthanum surface.

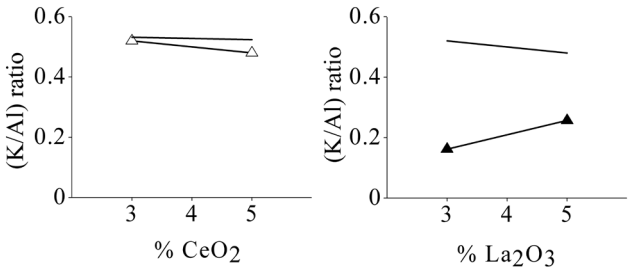

Figure 6. Atomic K/Al ratio: (-) bulk; (Δ) cerium surface; (▲) lanthanum surface.

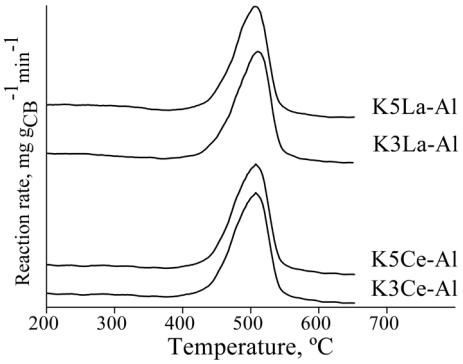

Figure 7. Curves of the carbon black combustion for the K-supported catalysts.

Table 4. Temperature at the maximum combustion rate, Tm and apparent activation energy for the K-supported catalysts.

Catalyst	Tm, ˚C	E act, kJ·mol^{-1}
K/3%CeO_2-Al_2O_3	480	81
K/5%CeO_2-Al_2O_3	480	92
K/3%La_2O_3-Al_2O_3	480	92
K/5%La_2O_3-Al_2O_3	470	92

for the K-supported catalysts; the larger decreases can be related to the redox and basic properties, favoring the oxygen activation on the catalyst surface.

4. Conclusion

The sol-gel method allows solids of high surface area to be obtained, thereby decreasing the area with the addition of potassium, which covers the pores of the material. The drastic effect is the most evident for the K/5%La_2O_3-Al_2O_3 catalyst. The effect of the incorporation of potassium increases its reducibility, decreases the surface area and allows having stronger oxygen in mixed oxides of a similar chemical nature. For K-La_2O_3 catalysts, La_2O_3 enters into the alumina and promotes the availability of K_2O in K/5%La_2O_3-Al_2O_3 with a chemical environment that favors its catalytic activity. However, for K-CeO_2 catalysts, the oxygen vacancies and mobility of these oxygen species for the catalytic activity in soot combustion reaction are crucial because the cerium oxide cannot enter the network. The characterization of the mixed oxides and K-supported catalysts confirms the importance of the use of potassium active phases as catalysts in soot combustion.

Acknowledgements

The authors would like to make special acknowledgements to FONDECYT, Grants 3150010 and 1130005, and Red Doctoral REDOC, MINEDUC Project UCO1202.

References

[1] Müller, J.O., Su, D., Jentoft, R.E., Wild, U. and Schlögl, R. (2006) Diesel Engine Exhaust Emission: Oxidative Behavior and Microstructure of Black Smoke Soot Particulate. *Environmental Science & Technology*, **40**, 1231-1236. http://dx.doi.org/10.1021/es0512069

[2] Pecchi, G., Reyes, P., López, T. and Gómez, R. (2004) Pd-CeO_2 and Pd-La_2O_3/Alumina-Supported Catalysts: Their Effect on the Catalytic Combustion of Methane. *Journal of Non Crystalline Solids*, **345&346**, 624-627.

[3] Dai, F., Zhang, Y., Meng, M., Zhang, J., Zheng, L. and Hu, T. (2014) Enhanced Soot Combustion over Partially Substituted Hydrotalcite-Drived Mixed Oxide Catalysts CoMgAlLaO. *Journal of Molecular Catalysis A*: *Chemical*, **393**, 68-74. http://dx.doi.org/10.1016/j.molcata.2014.05.031

[4] Thevenin, P., Alcalde, A., Pettersson, L., Järas, S. and Fierro, J.L.G. (2003) Catalytic Combustion Of Methane over Cerium-Doped Palladium Catalysts. *Journal of Catalysis*, **215**, 78-86. http://dx.doi.org/10.1016/S0021-9517(02)00146-X

[5] Ferrandon, M., Farrad, B., Björnbom, E., Klingstedt, F., Neyestanaki, A.K., Karhu, H. and Väyrynen, I.J. (2001) Copper Oxide—Platinum/Alumina Catalysts for Volatile Organic Compound and Carbon Monoxide Oxidation: Synergetic Effect of Cerium and Lanthanum. *Journal of Catalysis*, **202**, 354-366. http://dx.doi.org/10.1006/jcat.2001.3303

[6] Kundakovic, Lj. and Flytzani-Stephanopoulos, M. (1998) Cu- and Ag-Modified Cerium Oxide Catalysts for Methane Oxidation. *Journal of Catalysis*, **179**, 203-221.

[7] Pecchi, G., Cabrera, B., Buljan, A., Delgado, E.J., Gordon, A.L. and Jimenez, R. (2013) Catalytic Oxidation of Soot over Alkaline Niobates. *Journal of Alloys and Compounds*, **551**, 255-261. http://dx.doi.org/10.1016/j.jallcom.2012.10.015

[8] Pecchi, G., Reyes, P., Jiliberto, M.G., López, T. and Fierro, J.L.G. (2006) Catalytic Combustion of Ethyl Acetate over Ceria-Promoted Platinum Supported on Al_2O_3 and ZrO_2 Catalysts. *Journal of Sol-Gel Science and Technology*, **37**, 169-174. http://dx.doi.org/10.1007/s10971-005-6623-0

[9] Pecchi, G., Cabrera, B., Delgado, E.J., García, X. and Jimenez, R. (2013) Activity of $KNbO_3$ as Catalyst for Soot Combustion: Effect of the Preparation Method. *Applied Catalysis A*: *General*, **453**, 341-348. http://dx.doi.org/10.1016/j.apcata.2012.12.030

[10] Jimenez, R., García, X. and Gordon, A.L. (2010) About the Active Phases of KNO 3 /MgO for Catalytic Soot Combustion. *Reaction Kinetics*, *Mechanisms and Catalysis*, **99**, 281-287.

[11] Lox, E.S., Engler, B.H. and Koberstein, E. (1991) Diesel Emission Control. *Studies in Surface Science and Catalysis*, **71**, 291-321. http://dx.doi.org/10.1016/S0167-2991(08)62985-7

[12] Ahlstrom, A.F. and Odenbrand, C.U.I. (1990) Combustion of Soot Deposits from Diesel Engines on Mixed Oxides of Vanadium Pentoxide and Cupric Oxide. *Applied Catalysis*, **60**, 157-172. http://dx.doi.org/10.1016/S0166-9834(00)82179-X

[13] Fino, D., Fino, P., Saracco, G. and Specchia, V. (2003) Studies on Kinetics and Reactions Mechanism of $La_{2-x}K_xCu_{1-y}V_yO_4$ Layered Perovskites for the Combined Removal of Diesel Particulate and NO_x. *Applied Catalysis B*: *Environmental*, **43**, 243-259. http://dx.doi.org/10.1016/S0926-3373(02)00311-9

[14] Kureti, S., Weisweiler, W. and Hizbullah, K. (2003) Simultaneous Conversion of Nitrogen Oxides and Soot into Nitrogen and Carbon Dioxide over Iron Containing Oxide Catalysts in Diesel Exhaust Gas. *Applied Catalysis B*: *Environmental*, **43**, 281-291. http://dx.doi.org/10.1016/S0926-3373(02)00325-9

[15] Rahayu, S., Monceaux, W.L., Taouk, B. and Courtine, P. (1995) Catalytic Combustion of Diesel Soot on Perovskite Type Oxides. *Studies in Surface Science in Catalysis*, **96**, 563-574.

[16] Teraoka, Y., Nakano, K., Shangguan, W. and Kagawa, S. (1996) Simultaneous Catalytic Removal of Nitrogen Oxides and Diesel Soot Particulate over Perovskite-Related Oxides. *Catalysis Today*, **27**, 107-113. http://dx.doi.org/10.1016/0920-5861(95)00177-8

[17] Fino, D., Russo, N., Saracco, G. and Specchia, V. (2003) The Role of Suprafacial Oxygen in Some Perovskites for the Catalytic Combustion of Soot. *Journal of Catalysis*, **217**, 367-375. http://dx.doi.org/10.1016/S0021-9517(03)00143-X

[18] Shangguan, W., Teraoka, Y. and Kagawa, S. (1995) Effect of Oxide Composition of Spinel Type Cooper Chromites on the Catalytic Activity for the Simultaneous Removal NO_x and Soot Particulate. *Reports of the Faculty of Engineering*, *Nagasaki University*, **25**, 241-248.

[19] Uchisawa, J.O., Obuchi, A., Zhao, Z. and Kushiyama, S. (1998) Carbon Oxidation with Platinum Supported Catalysts. *Applied Catalysis B*: *Environmental*, **18**, L183-L187. http://dx.doi.org/10.1016/S0926-3373(98)00046-0

[20] Oi-Uchisawa, J., Obuchi, A., Enomoto, R., Xu, J., Nanba, T. and Kushiyama, S. (2001) Oxidation of Carbon Black over Various Pt/MOx/SiC Catalysts. *Applied Catalysis B*: *Environmental*, **32**, 257-268. http://dx.doi.org/10.1016/S0926-3373(01)00150-3

[21] Gross, M.S., Ulla, M.A. and Querini, C.A. (2009) Catalytic Oxidation of Diesel Soot: New Characterization and Kinetic Evidence Related to the Reaction Mechanism on K/CeO_2 Catalyst. *Applied Catalysis A*: *General*, **360**, 81-88. http://dx.doi.org/10.1016/j.apcata.2009.03.011

[22] Zhang, Z., Mou, Z., Yu, P., Zhang, Y. and Ni, X. (2007) Diesel Soot Combustion on Potassium Promoted Hydrotalcite-Based Mixed Oxide Catalysts. *Catalysis Communications*, **8**, 1621-1624. http://dx.doi.org/10.1016/j.catcom.2007.01.010

[23] Jimenez, R., García, X., Cellier, C., Ruiz, P. and Gordon, A.L. (2006) Soot Combustion with K/MgO as Catalyst. *Applied Catalysis A*: *General*, **297**, 125-134. http://dx.doi.org/10.1016/j.apcata.2005.08.042

[24] Jimenez, R., Garcia, X., Lopez, T. and Gordon, A.L. (2008) Catalytic Combustion of Soot. Effects of Added Alkali

Metals on CaO-MgO Physical Mixtures. *Fuel Processing Technology*, **89**, 1160-1168. http://dx.doi.org/10.1016/j.fuproc.2008.05.013

[25] Liu, J., Zhao, Z., Chen, Y.S., Xu, C.M., Duan, A.J. and Jiang, G.Y. (2011) Different Valent Ions-Doped Cerium Oxides and Their Catalytic Performances for Soot Oxidation. *Catalysis Today*, **175**, 117-123. http://dx.doi.org/10.1016/j.cattod.2011.05.023

[26] Li, Y., Gao, F., Kovarik, L., Peden, C.H.E. and Wang, Y. (2014) Effects of CeO_2 Support Facets on VOx/CeO_2 Catalysts in Oxidative Dehydrogenation of Methanol. *Journal of Catalysis*, **315**, 15-24. http://dx.doi.org/10.1016/j.jcat.2014.04.013

[27] Campbell, C.T. and Peden, C.H.F. (2005) CHEMISTRY: Oxygen Vacancies and Catalysis on Ceria Surfaces. *Science*, **309**, 713-714. http://dx.doi.org/10.1126/science.1113955

[28] Sawyer, R., Nesbitt, H.W. and Secco, R.A. (2012) High Resolution X-Ray Photoelectron Spectroscopy (XPS) Study of K_2O-SiO_2 Glasses: Evidence for Three Types of O and at Least Two Types of Si. *Journal of Non-Crystalline Solids*, **358**, 290-302. http://dx.doi.org/10.1016/j.jnoncrysol.2011.09.027

[29] Pecchi, G., Reyes, P., Zamora, R., López, T. and Gómez, R. (2005) Effect of the Promoter and Support on the Catalytic Activity of $PdCeO_{2-}$ Supported Catalysts for CH_4 Combustion. *Journal of Chemical Technology & Biotechnology*, **80**, 268-272. http://dx.doi.org/10.1002/jctb.1120

[30] Peralta, M.A., Milt, V.G., Cornaglia, L.M. and Querini, C.A. (2006) Stability of $Ba,K/CeO_2$ Catalyst during Diesel Soot Combustion: Effect of Temperature, Water, and Sulfur Dioxide. *Journal of Catalysis*, **242**, 118-130. http://dx.doi.org/10.1016/j.jcat.2006.05.025

[31] Mazumber, J. and de Lasa, H.I. (2014) Ni Catalysts for Steam Gasification of Biomass: Effect of La_2O_3 Loading. *Catalysis Today*, **237**, 100-110. http://dx.doi.org/10.1016/j.cattod.2014.02.015

[32] Dupin, J.C., Gonbeau, D., Vinatier, P. and Levasseur, A. (2000) Systematic XPS Studies of Metal Oxides, Hydroxides and Peroxides. *Physical Chemistry Chemical Physics*, **2**, 1319-1324. http://dx.doi.org/10.1039/a908800h

[33] Merino, N.A., Barbero, B.P., Grange, P. and Cadús, L.E. (2005) LaCaCoO Perovskite-Type Oxides: Preparation, Characterisation, Stability, and Catalytic Potentiality for the Total Oxidation of Propane. *Journal of Catalysis*, **231**, 232-244. http://dx.doi.org/10.1016/j.jcat.2005.01.003

[34] Zhao, Z., Yang, X. and Wu, Y. (1996) Comparative Study of Nickel-Based Perovskite-Like Mixed Oxide Catalysts for Direct Decomposition of NO. *Applied Catalysis B*: *Environmental*, **8**, 281-297. http://dx.doi.org/10.1016/0926-3373(95)00067-4

[35] Pecchi, G., Reyes, P., Zamora, R., Campos, C., Cadus, L.E. and Barbero, B. (2008) Effect of the Preparation Method on the Catalytic Activity of $La_{1-x}Ca_xFeO_3$ Perovskite-Type Oxides. *Catalysis Today*, **133-135**, 420-427. http://dx.doi.org/10.1016/j.cattod.2007.11.011

[36] Praveen, B.V.S., Cho, B.J., Park, J.G. and Ramanathan, S. (2015) Effect of La Doping of Ceria Abrasives for STI CMP. *Materials Science Processing*, **33**, 161-168.

[37] Fleming, P., Ramirez, S., Holmes, J.D. and Morris, M.A. (2011) An XPS Study of the Oxidation of Reduced Ceria-Lanthana Nanocrystals. *Chemical Physics Letters*, **509**, 51-57. http://dx.doi.org/10.1016/j.cplett.2011.04.090

[38] Sunding, M.F., Hadidi, K., Diplas, S., Løvvik, O.M., Norby, T.E. and Gunnæs, A.E. (2011) XPS Characterisation of *in Situ* Treated Lanthanum Oxide and Hydroxide Using Tailored Charge Referencing and Peak Fitting Procedures. *Journal of Electron Spectroscopy and Related Phenomena*, **184**, 399-409. http://dx.doi.org/10.1016/j.elspec.2011.04.002

[39] Haack, L.P., de Vries, J.E., Otto, K. and Chattha, M.S. (1992) Characterization of Lanthanum-Modified γ-Alumina by X-Ray Photoelectron Spectroscopy and Carbon Dioxide Absorption. *Applied Catalysis A*: *General*, **82**, 199-214. http://dx.doi.org/10.1016/0926-860X(92)85005-V

[40] Pecchi, G., Dinamarca, R., Campos, C.M., García, X., Jimenez, R. and Fierro, J.L.G. (2014) Soot Oxidation on Silver-Substituted $LaMn_{0.9}Co_{0.1}O_3$ Perovskites. *Industrial & Engineering Chemistry Research*, **53**, 10090-10096. http://dx.doi.org/10.1021/ie501277x